

N73-10524

164741

**Re-entry & Environmental  
Systems Division**

PHILADELPHIA, PENNSYLVANIA

STUDY OF FLUID MECHANICAL  
HELIUM-ARGON ION LASER

**CASE FILE  
COPY**

PROPERTY OF GENERAL ELECTRIC CO.  
MSD DOCUMENT CENTER  
VALLEY Forge Science Technology Center  
PHILADELPHIA, PENNA. 19161

GENERAL  ELECTRIC

STUDY OF FLUID MECHANICAL  
HELIUM-ARGON ION LASER

Contract No. NASW-1728

April 1972

Prepared for

NATIONAL AERONAUTICS AND SPACE ADMINISTRATION  
Office of Advanced Research and Technology  
Washington, D. C.

Environmental Sciences Laboratory  
Research and Engineering  
Re-entry and Environmental Systems Division  
General Electric Company  
Philadelphia, Pennsylvania

# CONTENTS

PAGE

LIST OF FIGURES	ii
FOREWORD	iii
ACKNOWLEDGMENT	iv
1. INTRODUCTION	1
1.1 Background and Concept Description	1
1.2 Scope of Investigation and Approach	4
2. ANALYSIS	6
2.1 Helium-Argon Ion Excitation	6
2.2 Argon Plasma Generation	9
2.3 Argon Plasma Expansion	9
2.4 Helium Injection	11
3. PRECURSOR EXPERIMENT	15
3.1 Description of Approach	15
3.2 Experimental Apparatus	15
3.3 Experimental Procedure	17
3.4 Results	18
4. ARC TUNNEL EXPERIMENT	20
4.1 Description of Approach and Experimental Facility	20
4.2 Injector Model	21
4.3 Gain Measurement	22
4.4 Results	24
5. SUMMARY	26
REFERENCES	28
FIGURES	30

## LIST OF FIGURES

PAGE

1.	Schematic of He-A <sup>+</sup> Laser Concept	30
2.	Energy Levels Pertinent to He-A <sup>+</sup> Laser	31
3.	Equilibrium Degree of Ionization as a Function of Pressure and Temperature for Argon	32
4.	Particle Concentration of Argon Plasma	33
5.	Degree of Ionization Against Area Ratio	34
6.	Ion and Electron Temperature	35
7.	Injection into Wake	36
8.	Stagnation Point Injection	36
9.	Injection Transverse to Flow	37
10.	Gain Measurement Apparatus	38
11.	Small Signal Gain vs. Pressure	39
12.	Diagram of Plasma Generator	40
13.	Arc Tunnel Gain Apparatus	41
14.	Schematic of Helium Injector	42
15.	Helium Injector in Arc Tunnel Test Section	43
16.	Schematic Diagram of Instrumentation	44

## FOREWORD

This document contains results obtained during the study supported by the NASA Office of Advanced Research and Technology under Contract NASW-1728.

The work was performed in the Environmental Sciences Laboratory, Dr. S. M. Scala, Manager - of the Research and Engineering Department, Re-entry and Environmental Systems Division, General Electric Company.

The principal investigator was J. S. Gruszczynski. He was supported by a team of specialists and technicians.

### ACKNOWLEDGMENTS

The author wishes to express his appreciation for the inspiring comments and encouragement given by Dr. S. M. Scala, Mr. R. J. Homsey, of this Laboratory and Dr. W. R. Warren presently with Aerospace Corporation. He also acknowledges the contributions by Dr. C. H. Marston, A. Clark, D. A. Rogers, N. S. Diaconis and R. Pridgen, in the experimental phase of this study and Mrs. D. Larkin for typing the text.

## 1. INTRODUCTION

### 1.1 Background and Concept Description

Following his postulate<sup>(1)</sup> of the possibility for population inversion on electronic states of gas particles Javan<sup>(2)</sup> demonstrated in 1961 the first successful gas laser in which electrically excited helium metastables were used to preferentially pump one of the higher energy levels of neon so that a population inversion was created and laser output could be obtained. In the ensuing years progress in the gas laser field continued at an ever-expanding rate. The number of identified laser transitions has increased from a few shortly after Javan's demonstration to thousands with the wavelengths at which laser oscillation were observed range now from ultraviolet to far infrared.

Much of this was straightforward, involving spectroscopic investigation of non-equilibrium gas states. However, the discovery of the lasing action between excited states of ions<sup>(3)</sup> in several noble gases resulting in the emission of highly coherent radiation throughout the visible range of the spectrum opened new areas for application of lasers. Subsequent development of the argon-ion laser led to a demonstration of both its pulse and CW operation. Although similar lasing action was observed in three other noble gases, the argon ion laser was found to be the most efficient.

Conventional electrically excited argon-ion lasers are characterized by the fact that the population inversion occurs between excited ion levels. Consequently very high current densities are required to produce the necessary degree of ionization and excitation in discharge plasma. It must be mentioned here that the main body of such argon-ion lasers is in a form of small bore diameter tube formed from a dielectric material or made from segmented and

insulated conductors which act as a constrictor for the discharge column. This tube is filled with essentially stationary argon gas through which the electrical discharge takes place. Excitation by rf power has also been reported<sup>(4)</sup>. The emission from the argon-ion laser is in the range between 4400 Å and 5200 Å where the existing detectors operate with high quantum efficiency. Thus it is an attractive candidate for many new applications such as deep space communication, space navigation and ultimately for wireless power transmission. Research and development studies<sup>(5,6)</sup> attempting to produce more power per unit volume of gas at increased efficiency concluded that further advancement in performance requires new approaches to overcome the problems with thermal loads associating with the waste heat generated in the process of excitation (including ionization) and with erosive action of the discharge on the confining structure. In the present state of the art the overall efficiencies (optical energy/input electrical energy) remain in the range of 0.1 percent and the CW power around 100 watts has been reported.

The solution to this problem was suggested by the development of the gas dynamic laser concept. This approach was derived from the experience gained in the laboratory investigations of aerothermodynamic phenomena associated with the hypersonic flight. In particular, fast expansion to high velocity of heated gases or plasmas in convergent-divergent nozzles was frequently plagued by a large departure from thermodynamic and chemical equilibrium. In order to understand the effects of non-equilibrium flows in the wind tunnels and their relation to the flight simulation a considerable research was conducted into the physical and chemical processes entering in the non-equilibrium flow phenomena. Potential application of the results of this research to new methods of producing population inversion between excited states of atoms or molecules

and enhancement of laser power output by mass convection has been recognized in 1962 by Hurle, Hertzberg and Buchmaster<sup>(7,8)</sup> in this country and independently by Basov and Oraevsky<sup>(9)</sup> in Russia. The most successful application of this concept has been in the case of the  $N_2-CO_2$  laser<sup>(10,11,12)</sup>.

An approach to an argon-ion laser based on the gasdynamic techniques has been the subject of the present study. It was expected that an appreciable improvement of the efficiency and power output could be achieved by eliminating the inherent drawbacks, such as high heat rejection problems and plasma confinement of the seal-off conventional lasers. In this scheme the process of producing population inversion between the same energy levels as in the conventional argon-ion laser, has been divided into two phases by separating from each other the processes of ionization and subsequent excitation. The ionization of argon is achieved in a conventional electric arc at pressures consistent with high efficiency of electrical energy conversion into gas enthalpy. During this process the gas is heated and ionized and its state is maintained in local thermodynamic equilibrium, LTE. This gas is then expanded to a supersonic velocity through a short convergent-divergent nozzle. Because of finite rates with which the recombination of electron and ions proceeds as the density and the kinetic temperature drop in the expanding flow, the degree of ionization lags behind that corresponding to the temperature of the heavy particles and the flow retains high electron density<sup>(13)</sup>.

The excitation of the upper laser level was to be achieved by resonant energy exchange, similar to that in helium-neon lasers<sup>(14)</sup>, between the triplet metastable helium atoms during mixing with the argon ions in the plasma flow. The excitation of helium metastables is carried independently from the argon

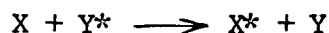
low levels of contamination of the test gas by the electrode and the constrictor plates materials<sup>(15)</sup>. Due to the differences in impedance between air arc and argon arc, the arc chamber had to be modified. During that period a precursor experiment was designed to investigate the energy exchange processes between the metastable helium and argon ions. This consisted of mixing a stream of rf generated argon plasma with a stream of rf excited helium. Small signal gain measurements were made along the axis of the mixing streams over a range of relative mass ratios and pressure levels.

Small signal gain measurements in arc tunnel with excited helium injection were performed using a wedge-shaped injector model. The injection was normal to the plasma flow. The length of the interaction zone was approximately 10 centimeters in the direction crosswise to the flow.

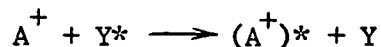
## 2. ANALYSIS

### 2.1 Helium-Argon Ion Excitation

Considering the very effective processes of energy transfer from long lived excited species of one gas to the lasing atoms or molecules of another, such as is the case of helium-neon<sup>(14)</sup> and nitrogen-carbon dioxide lasers<sup>(16)</sup>, respectively, we have examined a possibility of a metastable atomic state which would be suitable to preferentially pump upper laser levels of argon ions. In this approach we wanted to concentrate only on known laser transitions. It is known that in a system of two gases of which one has a metastable state very close in energy to an excited state in the second gas, a large cross-section is expected to exist for inelastic collisions, resulting in a transfer of excitation from an atom in the metastable state to the excited state of an atom of the second gas. This process is known as a collision of the second kind:



In the particular case of argon ions this can be written as:



In searching for the suitable partner in this reaction it was surprising to find that the  $2^3S$  helium metastable, the same species which participates in the helium-neon excitation, matches closely the energy levels of the upper laser level of argon ions.

A simple analysis indicates that providing the cross-section for the energy transfer between  $He(2^3S)$  and  $A^+$  is larger than the total cross-section of all other competing processes for draining the energy from the metastable level

and that the radiative life time of the 4p levels of argon ions is approximately ten times larger as measured<sup>(17)</sup> than the life time of the 4s levels, population inversion should be achieved.

Figure 2 shows a partial energy diagram pertinent to the studied scheme. We can see that the helium (<sup>3</sup>S) state closely coincides with the 4p levels of argon ions. A more detailed energy assignment is given in Table 1. Most of the argon ion states lie within kT (assuming T = 3000°K) with a minimum spread for the 4p<sup>2</sup>D<sup>0</sup> and 4p<sup>2</sup>P<sup>0</sup> configurations. Thus it is expected that these levels become selectively populated with respect to the 4s and 3d configurations which are too far removed from the helium metastable to be populated in a similar way.

An important factor, when the possibility of obtaining collisions of the second kind is investigated, is the Wigner spin rule<sup>(18)</sup>. This rule states that the excitation energy transfer is most probably when the total spin of the system is conserved. That is if the two series

$$\left| \begin{smallmatrix} \text{He} \\ S_i \end{smallmatrix} + \begin{smallmatrix} A^+ \\ S_i \end{smallmatrix} \right|, \left| \begin{smallmatrix} \text{He} \\ S_i \end{smallmatrix} + \begin{smallmatrix} A^+ \\ S_i - 1 \end{smallmatrix} \right|, \dots, \left| \begin{smallmatrix} \text{He} \\ S_i \end{smallmatrix} - \begin{smallmatrix} A^+ \\ S_i \end{smallmatrix} \right|$$

and

$$\left| \begin{smallmatrix} \text{He} \\ S_f \end{smallmatrix} + \begin{smallmatrix} A^+ \\ S_f \end{smallmatrix} \right|, \left| \begin{smallmatrix} \text{He} \\ S_f \end{smallmatrix} + \begin{smallmatrix} A^+ \\ S_f - 1 \end{smallmatrix} \right|, \dots, \left| \begin{smallmatrix} \text{He} \\ S_f \end{smallmatrix} - \begin{smallmatrix} A^+ \\ S_f \end{smallmatrix} \right|$$

have a common term. Here  $S_i$  and  $S_f$  are the initial and final spins respectively of the collision partners (helium and argon ions).

The ground state of argon ion is 3p<sup>5</sup>2P<sup>0</sup> and the ground state of helium is 2s<sup>1</sup>S<sup>0</sup>. Hence  $S_i^{\text{He}} = 1$ ,  $S_i^{A^+} = 1/2$ ,  $S_f^{\text{He}} = 0$  and  $S_f^{A^+} = 1/2$  for the doublet states or  $S_f^{A^+} = 3/2$  for the quartet states. Thus both the series reduce them-

TABLE 1. WAVELENGTH ALIGNMENT OF A<sup>+</sup> WITH He(3S)

Argon			Helium		$\Delta E = E_{\text{He}^*} - E_{\text{A}^+}^*$		
Designation	J	$E_{\text{A}^+}^*$ cm <sup>-1</sup>	Designation	$E_{\text{He}^*}$ cm <sup>-1</sup>	cm <sup>-1</sup>	ev	kT (T = 3000°K)
4p <sup>2</sup> S <sup>0</sup>	1/2	161090	3 2s <sup>3</sup> S	159850	-1240	-0.154	-0.596
	1/2	160240			- 390	-0.048	-0.187
4p <sup>2</sup> P <sup>0</sup>	3/2	159707			+ 143	+0.018	+0.069
	3/2	159394			656	0.081	0.314
4p <sup>2</sup> D <sup>0</sup>	5/2	158731			1119	0.138	0.534
	1/2	158429			1421	0.176	0.681
4p <sup>4</sup> D <sup>0</sup>	3/2	158168			1682	0.209	0.807
	5/2	157674			2276	0.282	1.090
	7/2	157234			2616	0.324	1.253

selves either to a single term  $1/2$  or to two terms  $3/2$  and  $1/2$ . Consequently there is a common term in each case and the Wigner rule is obeyed indicating a large probability for the excitation energy exchange. Although this rule applies in most cases departure from it are known.

## 2.2 Argon Plasma Generation

In the present study argon plasma is produced in a plenum chamber of an arc tunnel where cold argon is heated and ionized in an electric arc. At conditions of this study this process proceeds with the gas in local thermodynamic equilibrium. The corresponding degree of ionization of the plasma is closely related to its temperature and pressure as shown in Figure 3. For a high degree of ionization essential to a high power laser, plenum temperatures in excess of  $12,000^{\circ}\text{K}$  are required. As the temperature is increased doubly ionized argon will be produced as shown in Figure 4. However its particle density below  $T = 20,000^{\circ}\text{K}$  is small. Similarly equilibrium concentration of the  $4p$  states of  $\text{A}^+$  is negligible in the range between  $12,000^{\circ}\text{K}$  and  $20,000^{\circ}\text{K}$ . For instance at  $T = 14,500^{\circ}\text{K}$  the mole fraction of ions in  $4p$  states is approximately  $10^{-7}$ . Thus the possibility of obtaining a sizable population inversion by fast expansion and freezing of excited states similar to the  $\text{N}_2\text{-CO}_2$  gas-dynamic laser must be discounted.

## 2.3 Argon Plasma Expansion

It is known that when an ionized gas expands through a convergent-divergent nozzle from some predetermined initial conditions in a plenum chamber (pressure and temperature), it undergoes departure from equilibrium and so-called relaxation effects become important in determining the state of the gas at any given station along the nozzle. These relaxation effects arise

when the time required for a chemical reaction or atomic process is comparable with the transit time of the particle through the nozzle. In the rapid expansion of a partially ionized monatomic gas, such as argon, it is possible to distinguish two different modes of departure from equilibrium. In the first mode, it is expected that if the three-body process is the dominant mechanism for recombination, the temperature of the electron gas will be considerably higher than the atom-ion temperature. This is due to the large mass ratio between atoms and electrons which requires very many collisions to distribute the energy between the light and heavy particles. Very closely associated with this effect is the second mode; the so-called chemical non-equilibrium, that is, the departure of electron particle density from the values calculated with the Saha relations. This type of non-equilibrium flow was a subject of many theoretical and experimental investigations<sup>(13,19,21)</sup>. A comprehensive theoretical study of the non equipartition of energies and chemical non-equilibrium in a supersonic nozzle flow of argon gas was made by Bray<sup>(13)</sup> for the case of a Maxwellian temperature distribution of electrons. Results of this study are used here to predict flow properties in expanded arc tunnel flow.

Briefly, Bray's theoretical treatment relies on the assumption that the de-ionization rate is limited by the de-excitation and by the removal of energy released in recombination by electrons. This leads to recombination rate increasing with falling electron temperature and to an electron temperature considerably in excess of the ion-atom temperature. Figure 5 shows representative results from these calculations for a plenum temperature of 16,400°K and a plenum pressure of 0.56 atmospheres. The degree of ionization is plotted here as a function of nozzle area ratio  $A/A^*$ , where  $A^*$  is the throat area. The corresponding electron and heavy particles temperature is shown in Figure 6. Since

the transit time of the atom through the nozzle determines the degree of the departure from equilibrium, the throat size and the nozzle divergence angle are important parameters in predicting the expanding flow properties.

#### 2.4 Helium Injection

Several possible schemes of injection of the helium metastables into the stream of flowing argon plasma were analyzed in order to arrive at a configuration which would offer rapid mixing between these two gases thereby creating the environment for the energy exchange between the metastable helium ( $2^3S$ ) state and the ground level of argon ions. The velocity of diffusion is a critical consideration since it will determine the rate of energy exchange and hence the power extraction.

This requirement dictates the necessity to create breakdown of the laminar flow to supplement and augment the natural molecular diffusion driven by the concentration gradients between these two gases. It is also known that large velocity discontinuities, shear layers, which can exist between the main stream and the injected gas are inherently unstable. This phenomena can be expected to promote mixing. In addition, it is desirable to have a large contact area between the two gases to speed up the diffusion process.

At first an approach as shown in Figure 7 has been considered. It consists of a manifold injecting into its wake region. In this configuration the velocity of the injected gas is considerably lower than the velocity of the external flow, creating large velocity gradients along the contact streamline as is shown in Figure 7. Assuming a simple, one-dimensional diffusion model and using a binary diffusion coefficient for He-Ar mixture of  $D_{12} = 0.65 \text{ cm}^2/\text{sec}$ ,

the result indicates that the centerline concentration - along the wake will decrease to 25% of its initial value in a distance of approximately 10 cm. It should be noted that because of its low molecular weight helium diffuses about four times faster into argon than nitrogen into oxygen at the same pressure and temperature. In the consideration of the wake diffusion it was assumed that the diffusion coefficient varies

$$D_{12} \propto \frac{T^{3/2}}{p}$$

where T is the temperature and p the pressure. No allowance was made for the diffusion due to temperature gradients which in the case of low temperature of helium and much higher temperature of argon plasma can speed up the diffusion by an appreciable amount. Observation of similar effects in the wake diffusion processes (slender body in supersonic flight) reported in Ref. 22 in which also the effect of turbulent mixing were shown to change dramatically the characteristic diffusion time. In the present case it was not expected that the transition to turbulent flow in the wake will take place due to a relatively small Reynolds number (of the order of 10/cm) in spite of a high velocity along the separation streamline. A comparison of the anticipated performance of this approach was made with two alternate configurations which are shown in Figure 8 & 9. One of these represents a forward facing jet. A number of investigators have considered the problem of injection at the forward facing stagnation point. The results of the recent studies are reported in Refs. 23 and 24. They were able to classify two distinct types of jet interaction for the free stream flow, depending on the total pressure ratio between the jet and the free stream. In the subsonic interaction case the bow shock is moved away from the body. The mixing which occurs along the interface streamlines is mainly due to molecular

diffusion. A more interesting case is one which involves not only the shock displacement but also produces a significant shape change and unsteadiness. The breakdown of the blunt interaction and the establishment of a spike interaction occurs when the total pressure in the jet and free stream do not match. The unsteady behavior of the flow is beneficial to the present application by promoting mixing between the injected helium and the argon plasma.

The more attractive method considered here is shown in Figure 9. It uses a flat plate with a sharp leading edge which can be tilted to any desired angle of attack. Helium is injected through a series of orifices located on the surface of the flat plate away from the leading edge. This configuration is similar to that studied in Ref. 25 except for the method of injection and the symmetry of the wedge. The injection method of Ref. 25 employed porous surface to produce massive blowing, which strongly affected both the boundary layer and the position of the shock. This method however is not suitable for injection of excited helium atoms because of the strong effects of walls on the lifetime of the metastables. An alternate approach is to inject helium through a series of discrete jets, thus satisfying the requirements of large contact area for the contact surface between helium and argon plasma and large velocity gradients to produce enhancement of mixing by the laminar flow breakdown. Changing the angular orientation of the flat plate could be used to alter the flow pattern and optimize the interaction between helium metastables and argon plasma.

In the case of operation with the injection manifold at a negative angle of attack no sharp discontinuity with the Rankin-Hugoniot structure is formed because of the relatively low pressure. Instead a diffused oblique shock with

an appreciable thickness appears over the upper surface of the flat plate. A result of this interaction is to increase the shock wave angle and hence the pressure ratio over that corresponding to the Rankin-Hugoniot pressure behind an oblique shock wave for a given wedge angle<sup>(26)</sup>.

### 3. PRECURSOR EXPERIMENT

#### 3.1 Description of Approach

During the period of evaluation of the arc tunnel performance with argon as the working fluid (all previous operation of this facility was with air) and calibration of the flow properties a precursor experiment was designed in order to proceed with the investigations of the excitation of argon by means of energy exchange with helium metastables. The approach selected here was to use rf excitation to produce argon plasma and to excite helium. The requirement was to perform small signal gain measurements over a range of pressure and mole fraction of the gas mixture. This could be accomplished by exciting separately each of the gases and then bringing them together to mix. To assure rapid mixing the excited gases are brought together in the form of two impinging jets at the center of a mixing tube from where they flow along the optical axis towards the exit tube.

#### 3.2 Experimental Apparatus

This investigation was carried out in the experimental apparatus shown schematically in Figure 10. The interaction tube was formed from one-inch diameter Pyrex pipe of 24 inches total length. The return loop extended 10.5 inches on either side of the two injection nozzles which were located across from each other at the center of the interaction tube. The end of this tube were closed-off with quartz windows. The diameter of injector tubes was 0.4 inches.

The return loop outlet was connected to a large dump tank (approximately 150 cubic feet volume) through a throating valve which was used to set the pressure of the gas mixture in the reaction tube. Initially the outlet was connected directly to a large vacuum pump but it was found that the flow in the

reaction tube was not steady and that the flow pulsations produced by the operation of the vacuum pump were transmitted to the test section. Two multiple-turn air core coils with their axis parallel to the axis of the injector tubes and connected in parallel to the constant frequency 12 MHz exciter were used to couple the rf energy to the flowing gases. The exciter power was regulated by controlling current in the primary circuit of the oscillator. High purity grade helium and argon were used. The flows were measured by Fisher and Porter flow-rators and could be adjusted by means of needle valve to give any desired mass flow ratios.

The gain measuring system consisted initially of a CW hv-system Inc. argon-ion laser. The output of the laser was chopped at 60 cycle per second and expanded to a beam of 0.5 inch diameter. A 50%-50% beam splitter was used to direct part of the laser output to a monitor detector. The other part was sent through the quartz window along the axis of the interaction tube. After passing the interaction tube the beam was detected by an EMI photomultiplier with S20 cathode response characteristics.

Shortly after the start of the experiments the laser failed to emit and had to be returned to the manufacturer. After two repairs it was decided that the problem is caused by faster than usual diffusion of ions into the capillary walls while the plasma is generated. The drop in gas pressure or lack of laser emission was reflected in the inability of the plasma tube to ignite.

A modification of the laser was undertaken which consisted in providing access to the gas reservoir. Thus it was possible to refill the tube with a fresh charge of argon and adjust the gas pressure in the plasma tube for optimum

operation of the laser. A refill station was constructed which included ion vacuum pump which allowed us to evacuate the plasma tube down to  $10^{-5}$  millimeter pressure before refilling the tube with research grade argon. Unfortunately this involved manipulation of two valves which could easily break off even with the application of a small force. After one such failure a decision was made to purchase a TRW Model 83A pulsed argon ion laser. The experimental arrangement remained essentially unchanged except for the chopper which was not needed.

Side emission from the mixing region of helium and argon was monitored with Heath EU-700 scanning monochromator. This instrument has a  $f/6.8$  aperture and a reciprocal dispersion of  $20 \text{ \AA}^{\circ}$  per millimeter. The signal detection was made with an RCA 1P28 photomultiplier (S5 cathod response characteristic) and recorded on a Tektronix 535 dual beam oscilloscope.

### 3.3 Experiment Procedure

At the beginning of each test run the dump tank was evacuated to approximately 50 microns and kept at this pressure during the test by continuous pumping. The pressure in the interaction tube was adjusted by opening the micrometer valves in the individual gas lines and adjusting the relative flow of helium and argon to obtain the desired gas flow ratio. The experimental conditions extended over a range of mixture pressures between 0.5 and 10 torr and it was varied in steps of 0.5 torr. The mole ratio of helium and argon,  $\psi = M_{\text{He}}/M_{\text{Ar}}$ , was kept constant at each pressure. To evaluate the effect of the mixture the mass flow of each gas was varied so as to obtain a range of  $\psi$  between 0.10 and 10 thus covering a wide range of possibilities. The corresponding through flow velocities in the interaction tube were 50 to 500 ft/sec. After adjusting the desired pressure and flow conditions the rf excitation was switched on and the gain

using the probe laser was measured. Prior to the gain measurements, the side radiation was scanned with the Heath scanning monochromator in order to establish the presence of metastable helium atoms and argon ions in the mixing zone. During the experiments it was found that no cooling of the interaction tube was necessary due to the rapid convection of the excited gas. With the beam expanded to approximately 1 centimeter diameter the measurements were made only along the axis of the tube. The excitation power was set at 100 ma current flow in the primary circuit which corresponded to maximum coupling between the rf field and the gas.

### 3.4 Results

The experimental data obtained during this phase of the study are summarized in Figure 11. The initial measurements were made with the CW argon-ion laser using an internal Litrow prism for wavelength selection. The data indicate a considerable scatter and it was not possible to develop a constant trend. Some of the measurements suggested a small gain with  $\alpha = 0.1$  at the  $4880 \text{ \AA}$  wavelength over a range of pressures between  $p = 0.8$  and  $p = 1.5$  torr. It was not possible to complete this scheduled test matrix due to failure of the laser.

As was mentioned earlier the laser was returned to the manufacturer for repairs. Eventually it was found that a rapid loss of the gas in the plasma tube was the main reason for the failures and provisions were developed to refill the tube as needed in the laboratory without loss of time in shipment to the manufacturer.

The remainder of the tests were done with the pulsed argon-ion laser

which was found to put out much more repeatable pulse intensity at both wavelengths ( $4880 \text{ \AA}$  and  $5145 \text{ \AA}$ ). Since the laser was not equipped with internal means for wavelength selection interference filters were used to isolate the required lines. Measurements were also made with probe laser oscillating on all lines.

Figure 11 shows a plot of obtained gain data as a function of total gas pressure with both the CW and pulsed lasers. Filled symbols represent data taken with the CW laser. It can be seen that within the accuracy of the test data there is no amplification of the probing signal in its passing through the mixing region in the interaction tube.

Analysis of the residence time in tube shows ample time for the energy exchange to occur. For instance, at  $p = 1$  torr and helium mass flow of  $0.1 \text{ gram/sec}$  assuming the temperature to remain at  $T = 300^\circ\text{K}$  the residence time is approximately  $5 \times 10^{-3}$  seconds.

Spectral observations indicated presence of helium metastables ( $\text{He}(2^3\text{S}) - 3889 \text{ \AA}$  and  $\text{He}(2^1\text{S}) - 5016 \text{ \AA}$ ). Presence of ionized argon was indicated by lines at  $4348 \text{ \AA}$  and  $4764 \text{ \AA}$ .

#### 4. ARC TUNNEL EXPERIMENT

##### 4.1 Description of Approach and Experimental Facility

The fundamental feature of the present approach is to separate the processes of ionization (plasma production) from each other. The plasma production is accomplished continuous flow arc heater where cold argon is heated and ionized in an arc burning between two carbon electrodes as shown in Figure 12. This particular heater with tandem-Gerdien arc configurations has been extensively used in the past as a plasma source in aerodynamic and material studies. Diagnostic investigations conducted in the course of these studies confirmed that it is possible to produce gas flows with low levels of contamination by the electrode material. At pressures between 0.1 and higher, the plasma in the arc heater plenum chamber has been shown to be in LTE with the gas temperature (enthalpy) controlled by electric power input up to  $10^6$  watts.

After heating in the plenum chamber argon plasma is expanded through a 5/32 inch diameter throat into the divergent section with an overall area ratio of  $A/A^* = 971$  where  $A^*$  is the throat area. The exit diameter of the jet was 4.9 inches. The helium injector flat plate model was located in the test section. Being mounted through the side window of the tunnel the flat plate could be set at any desired angle of attack with respect to the plasma flow by rotation of the support sting, as illustrated in Figure 13. At 30 degree angle the leading edge of the model was located 0.5 inches from the exit plane of the nozzle. In this orientation the position of the orifices was on the center line of the nozzle. Rotation by 15 degrees results in raising the position of helium injection orifices approximately 0.2 inches above the center line of the nozzle. This displacement is considered to be insignificant regarding the variation of

plasma conditions in the transverse direction. The test section is provided with large windows on both sides of the tunnel permitting viewing of the complete flow field between the nozzle exit plane and the diffuser inlet. These windows were also used for the probe beam passage. The test section pressure was maintained at a level of 100 microns by continuous pumping by a 5500cfm mechanical vacuum pump system.

#### 4.2 Injector Model

Model for injection of the excited helium into the stream of high velocity nonequilibrium (degree of ionization of the plasma frozen at a temperature close to the plenum conditions) argon plasma is shown in Figure 14. It consists of the following parts. The main body is a boron nitride flat plate (0.25 inch thick, 7.5 inch wide and 3.5 inch long) with a pyrolytic graphite section forming a sharp leading edge (10 degree included angle). The injection manifold was bonded to the underside of the plate in a recess so that the effective wall thickness separating the inside of the manifold from the upper surface of the flat plate was kept to approximately 0.032 inches. A total of 34 orifices, equally spaced at 0.125 inches were drilled through the plate and the manifold. Their diameter was 0.032 inches. The manifold was made of boron nitride 1-inch tubing which was placed between two aluminum plates forming the capacitance load of the rf exciter. The injection manifold and the capacitor plates were enclosed in a vacuum tight box attached to the flat plate to allow higher pressure to exist there which was found necessary to prevent arcing. The model was sting-mounted (Figure 15) through the side window of the tunnel. The hollow sting, opened to the atmosphere, was also used to bring in the rf exciter power leads which also had to be kept at atmospheric pressure to prevent

dissipation of power in the corona discharge at the tunnel operating pressure level. A helium supply line was connected directly to the injection manifold in the arc tunnel test section. The rate of flow of helium was measured using Fisher and Porter Tri-Flat flow rator. Manifold pressure was measured using a Heise gage located at the entry to the injector manifold. Standard grade helium was used throughout the experiment.

#### 4.3 Gain Measurement Instrumentation

The apparatus arrangement for gain measurement is shown in Figure 16. It consists of a TRW Model 83A pulse argon laser operating in a single mode ( $TEM_{00}$ ) with a pulse repetition rate corresponding to the line frequency (60 pps) and an internal trigger. The pulse width is approximately 6 microseconds at the 50% intensity points. The output beam is expanded to approximately 2 cm and then apertured down to 0.1 cm so that only the central part of the beam with uniform intensity distribution is allowed to enter the test section and is used for diagnostics. The beam is then split by 50%-50% beam splitter. One part of the beam is directed to the monitor detector while the other passes through the arc tunnel test section over the flat plate model. A second aperture limits the unwanted spurious radiations generated in the test section of the tunnel. A narrow bandpass filter was used to isolate the  $4880 \text{ \AA}^0$  transition of argon ions at the entrance to the gain detector on the other side of the test section.

In arriving at a satisfactory set-up of the optical configuration it was recognized that the problem of refraction effects caused by flow inhomogeneities, and optical feedback may seriously affect the measurements. Density gradients, transverse to the optical axis, produced by the expansion nozzle can cause a significant deflection of the beam. This deflection may cause the

section of the beam previously incident on the detector to shift off the sensor, while rays previously not intercepted by the detector may be detected. This may change the recorded signal independently of the amount of optical gain in the reaction zone. The approach adopted here makes use of utilizing a beam diffuser in front of the detectors. Ideally one would prefer to have a perfectly homogeneous Lambertian reflector. The beam incident on such a surface will scatter while the detector is sensing fractions of the scatter radiation. It can be shown that the amount of radiation reaching the detector is insensitive to small wander of the beam on the scattering surface thus removing the problems associated with diagnostic beam refraction. The best diffuser was found to be sand-blasted aluminum which was selected for use in the present experiments. To avoid feedback into the diagnostic laser by reflection from windows and filters, the beam axis was inclined slightly to the reflective surfaces.

Laser beam monitoring and gain measurement was made with an RCA 929 vacuum photodiodes which have S-4 response characteristics. A 2-mm aperture was placed in front of the detectors to reduce the amount of light incident on the photocathode. Both detectors viewed directly the reflecting diffuser surface.

The detectors were powered by a 90 volt battery and the output was read across a 470 ohm resistor. The signals were displayed on Tektronix 545 dual-beam oscilloscope with 1A7 plug-in preamplifiers which combined with low capacitance cables had submicrosecond response time with low noise characteristics.

The gain measuring detector viewed the laser beam through interference filters manufactured by Thin Film Products, Inc., with peaks at 4880 Å and

5145 Å and half width of approximately 10 Å.

#### 4.4 Results

All of the past experience in the operation of the ESL arc tunnel facility was with air as the working fluid. It was therefore necessary to expend a considerable effort in characterizing its performance in argon. The first difficulty encountered was the electrical power supply which was designed to operate at voltage and current levels consistent with the impedance of air plasma. Operation with argon called for a considerably lower voltage and thus the external ballast resistor and the associated circuitry had to be changed to match argon plasma impedance. Initial calibration were made at plenum pressures above one atmosphere using water cooled calorimeters for measuring total enthalpy.

In addition simultaneous spectrographic observations were made of the gas at the exit from the plenum chamber. The results showed a very low degree of ionization and nitrogen contamination of plasma. Low temperature of the argon plasma as compared to air plasma was also traced to the electrical characteristics of argon. To remedy this, two steps were taken. First, the plenum pressure was reduced below atmospheric, and second, the arc was lengthened to allow argon to pass through a longer column and thus acquire more energy from the arc discharge. Using a small plenum chamber, new measurements with these improvements indicated temperatures in the throat of approximately 13,000°K and a degree of ionization of about 0.4. As a next step total pressure probe and Langmuir probe traverses were made in the nozzle exit plane to establish plasma jet properties. These measurements were found to be consistent with the calorimetric data.

All tests with the helium injector were made at 20 degree angle of attack of the model flat plate. The probing with the beam from the pulsed argon-ion laser extended over the mixing region as indicated in Figure 14. The difference between the readings without rf excitation and with it represents either absorption or gain produced by the interaction of the excited helium and argon plasma. Care was taken to allow for any change in beam intensity between different pulses. The principal variable was the pressure in the helium manifold which essentially determined the total mass of injected gas. The pressure extended from 5 to 25 torr while the static pressure on the surface of the flat plate model ahead of the injection orifices was measured to be 1 torr. Thus helium jets were underexpanded, the final expansion occurring outside the orifices. A very careful examination of all the data did not reveal any presence of gain thus indicating that no energy exchange between excited helium and argon ions leading to the preferential population of the upper levels of the ion was taking place.

## 5. SUMMARY

The subject of the present study was a new concept of a gas laser which emits in the visible part of the wavelength spectrum. In particular the study addressed itself to the experimental investigations of the feasibility of a new approach to an argon-ion laser. This approach involves gas dynamic methods to produce ionized plasma and subsequent mixing with rf discharge generated helium atoms in the triplet metastable state which served for the upper laser level pumping mechanism. By a fast flow of the active medium through the laser cavity power levels considerably higher than those obtained in conventional sealed-off lasers are predicted. Up to one watt per cubic centimeter can potentially be produced. The overall efficiency being strongly affected by the low quantum efficiency of the argon-ion laser transitions ( $\eta_q = 7.2\%$ ) was predicted to be above one percent.

Small signal gain measurements were performed in two experimental configurations. One involved subsonic mixing of rf produced argon and helium plasmas. The second configuration consisted of an arc tunnel in which equilibrium argon plasma was generated in a dc arc and subsequently expanded into a test section. Independently excited helium was injected into the fast flowing frozen plasma.

The measurements covered a wide range of conditions and were made with a conventional argon-ion laser. The data so obtained showed no amplification of the probe signal indicating absence of population inversion. Apparently, competing processes drain energy from the helium metastables at a higher rate than that of the resonant transfer to the argon-ion upper laser

level. Since the ionization potential of argon is lower than the excitation energy of the metastable state of helium ( $2^3S$ ) it is suspected that so-called Penning effect dominated the energy exchange.

It is suggested that the resonant energy transfer process between argon ions and the triplet helium state should be evaluated under closely controlled conditions. A shock tube could be used to produce highly ionized argon plasma and serve as a source of ions into which excited helium is introduced.

## REFERENCES

1. Javan, A., "Possibility of Production of Negative Temperature in Gas Discharges", Physical Review of Letters, 3, 87-89 (1959).
2. Javan, A., Bennett, W. R., Jr., and Herriott, D. R., "Population Inversion and Continuous Optical Maser Oscillation in a Gas Discharge Containing a He-Ne Mixture", Physical Review of Letters, 6, 106-110 (1961).
3. Bridges, W. B., Applied Phys. Letters, 4, 128-130 (1964).
4. Goldsborough, J. P., Hodges, E. B., and Bell, W. E., "RF Induction Excitation of CW Visible Laser Transitions in Ionized Gases", Applied Physics Letters, 8, 218-219 (1966).
5. Labuda, E. G., Gordon, E. I., and Miller, R. C., "Continuous-Duty Argon Ion Lasers", IEEE J. Quantum Electronics, QE-1, 273 (1965).
6. Paananen, R. A., "Progress in Ionized-Argon Lasers", IEEE Spectrum, (1966).
7. Hurle, I. R., Hertzberg, A., and Buckmaster, J. D., "The Possible Production of Population Inversions by Gasdynamic Methods", CAL Report No. RH-1670-A-1, (1962).
8. Hurle, I. R., and Hertzberg, A., "Electronic Population Inversions by Fluid-Mechanical Techniques", Physics of Fluids, 8, 1601 (1965).
9. Basov, N. G., and Oraevskii, A. N., "Attainment of Negative Temperatures by Heating and Cooling of a System", Soviet Physics-JETP, 17, 1171-1274 (1963).
10. Konyukhov, V. K., and Prokhorov, A. M., "Population Inversion in Adiabatic Expansion of a Gas Mixture", JETP Letters, 3, (1966).
11. Basov, N. G., Oraevskii, A. N., and Shcheglov, V. A., "Thermal Methods for Laser Excitation", Soviet Physics-Technical Physics, 12, 243-249 (1967).
12. Gerry, E. T., "Gas Dynamic Lasers", IEEE Spectrum, 7, 51-56 (1970).
13. Bray, K. N. C., "Electron-Ion Recombination in Argon Flowing through a Supersonic Nozzle", Proceedings AGARD-NATO Specialists Meeting, Rhode-Saint-Genese, Belgium, 67-87, (1962).
14. Javan, A., Bennett, W. R., and Herriott, D. R., "Helium-Neon Laser", Phys. Rev. Letters, 6, 106 (1961).

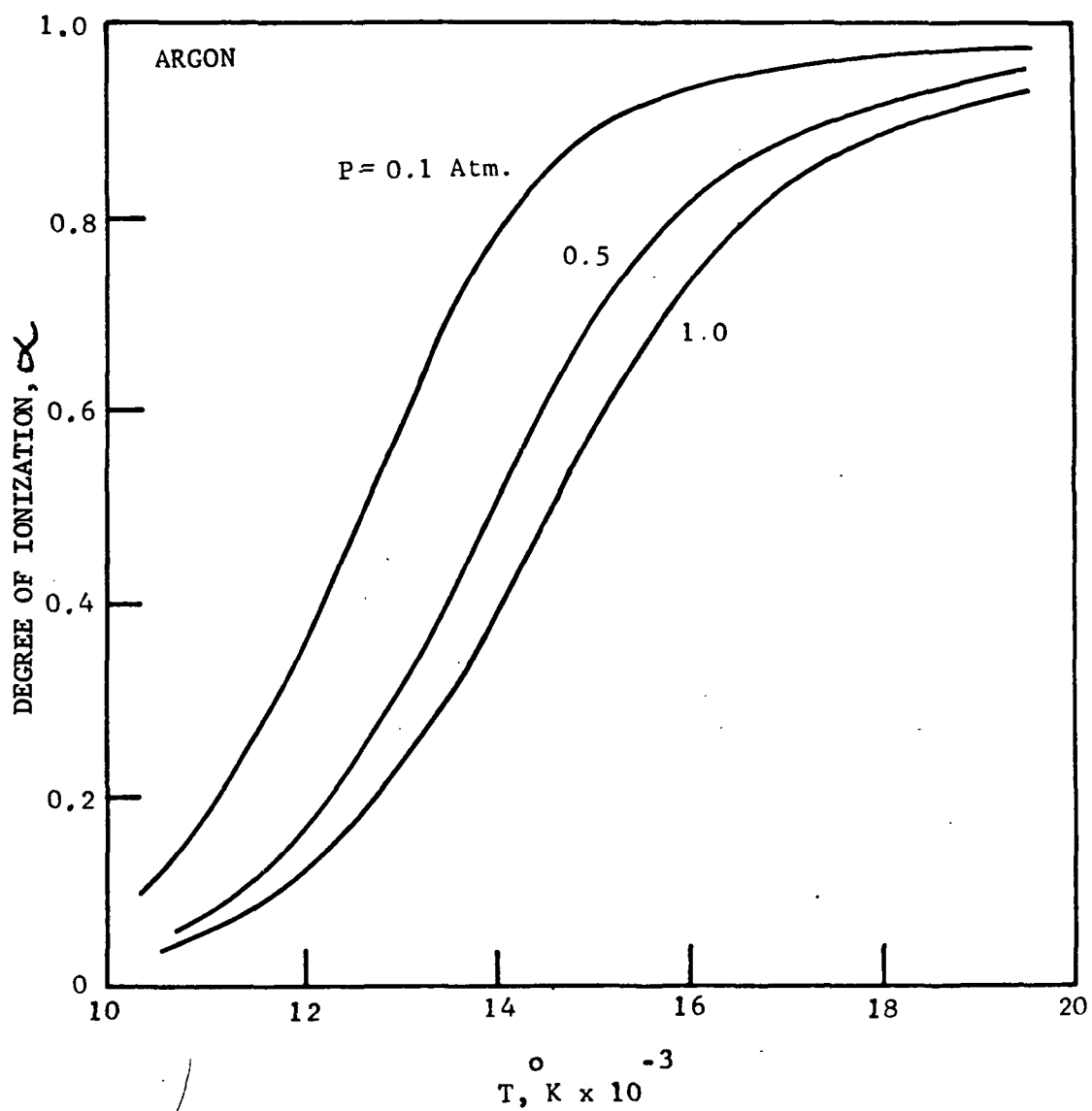
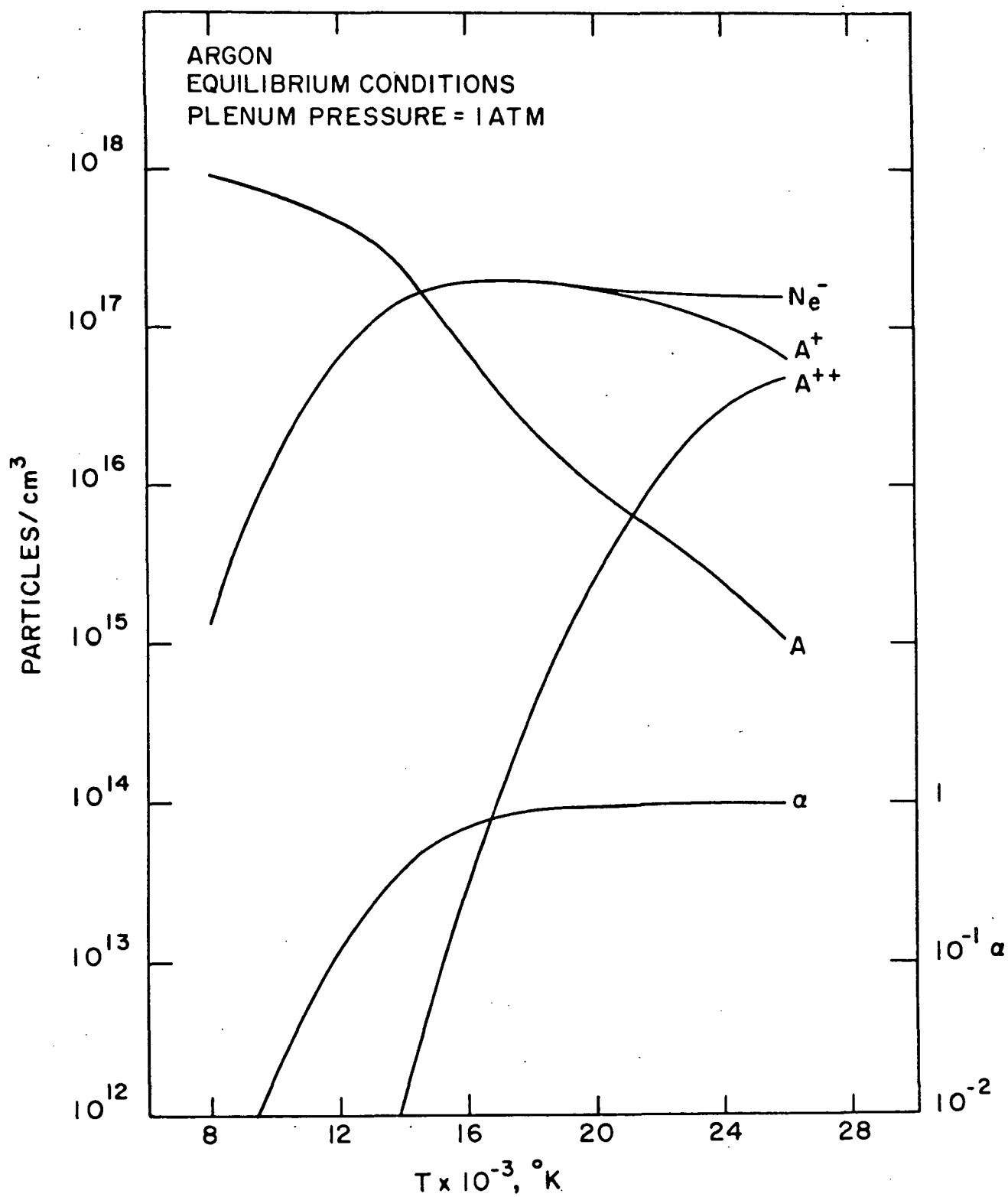


Figure 3 Equilibrium Degree of Ionization As A Function of Pressure And Temperature For Argon



N103-646

Figure 4. Particle Concentration of Argon Plasma

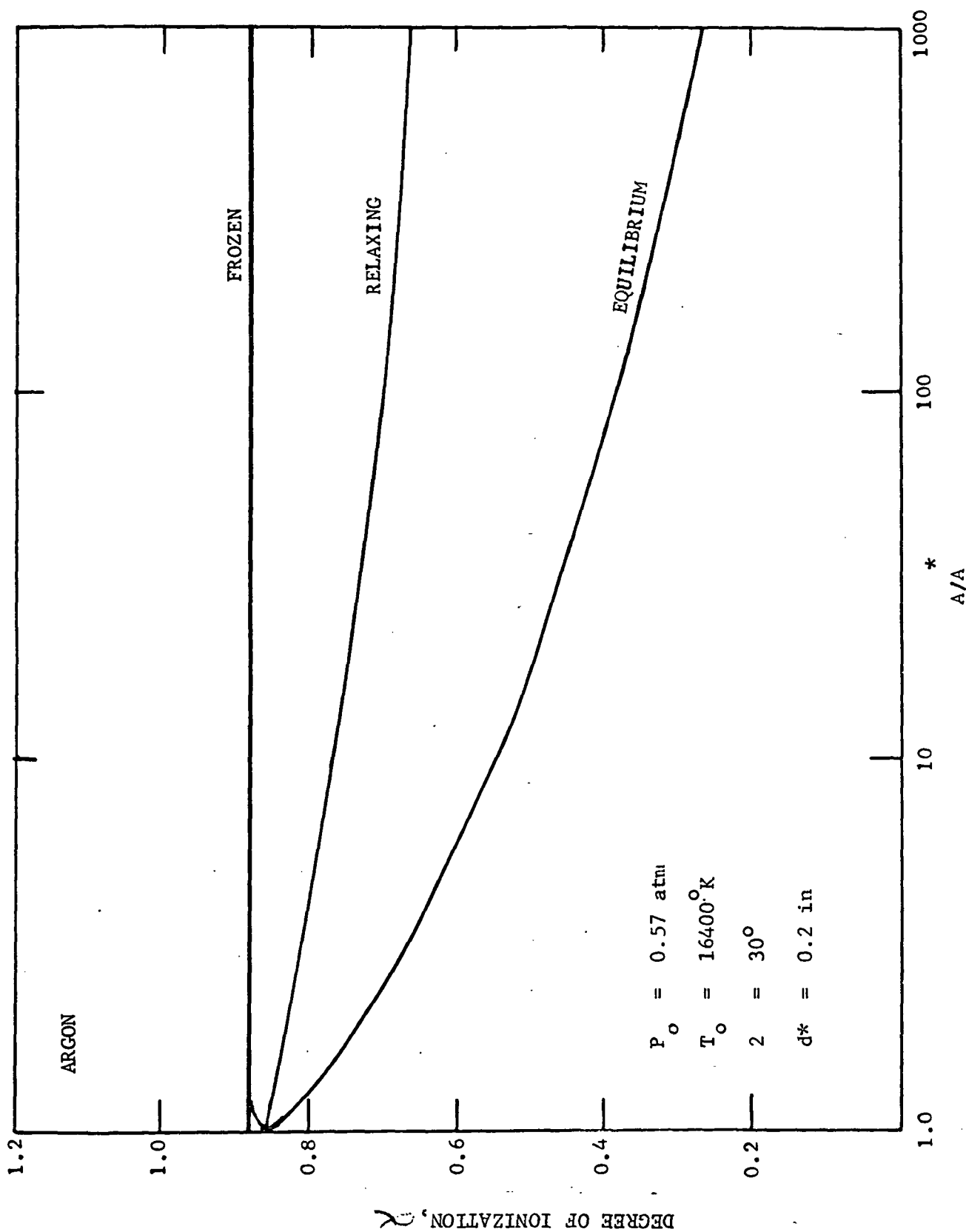


Figure 5 Degree of Ionization Against Area Ratio

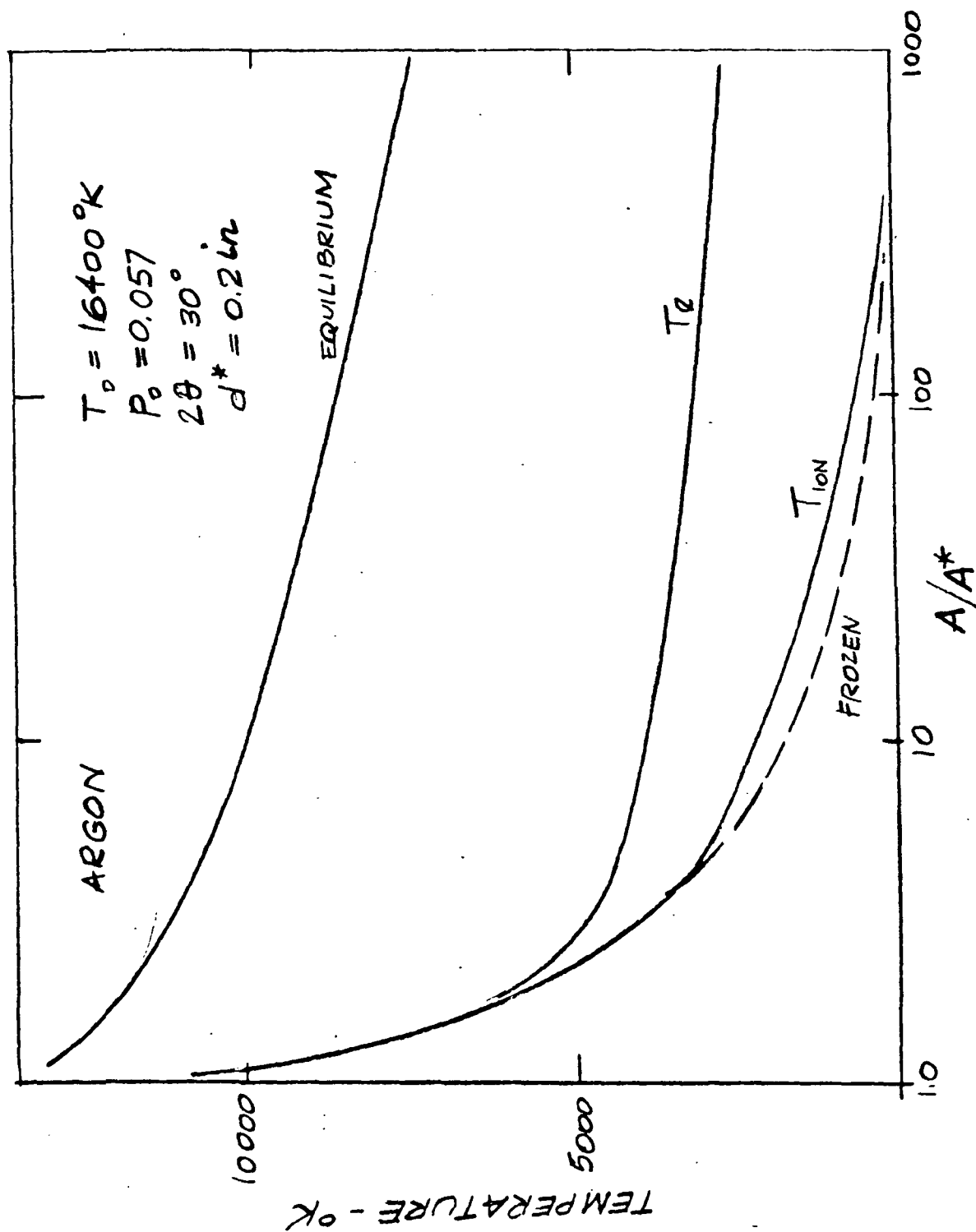


Figure 6. Ion and Electron Temperature

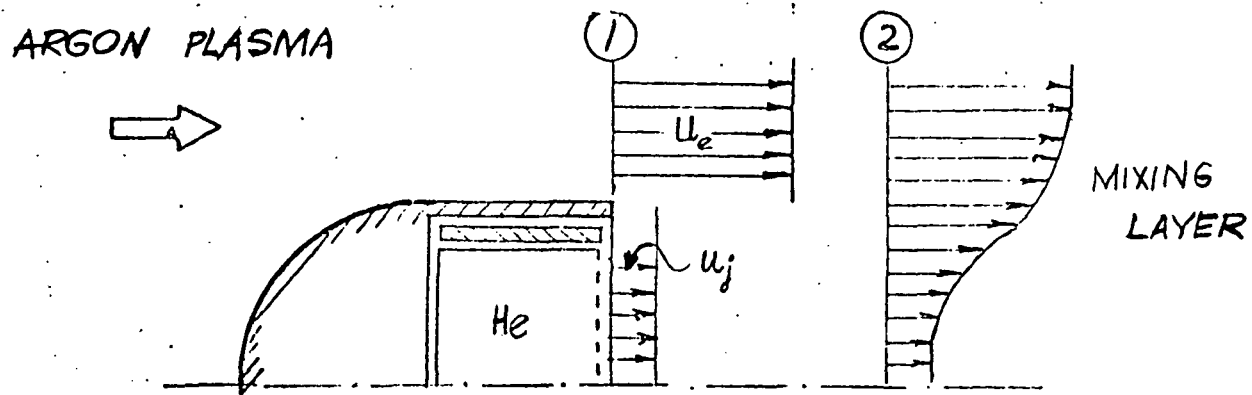


Figure 7. Injection into Wake

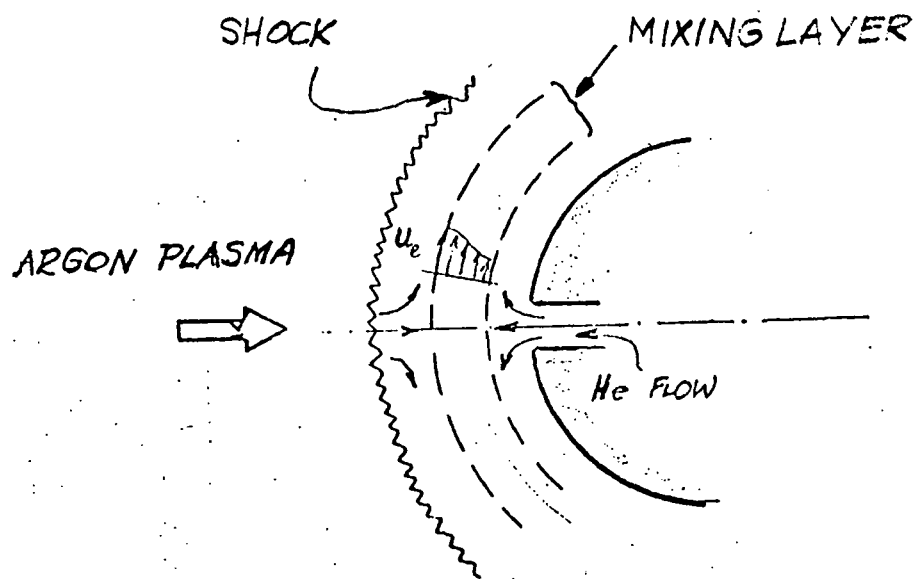


Figure 8. Stagnation Point Injection

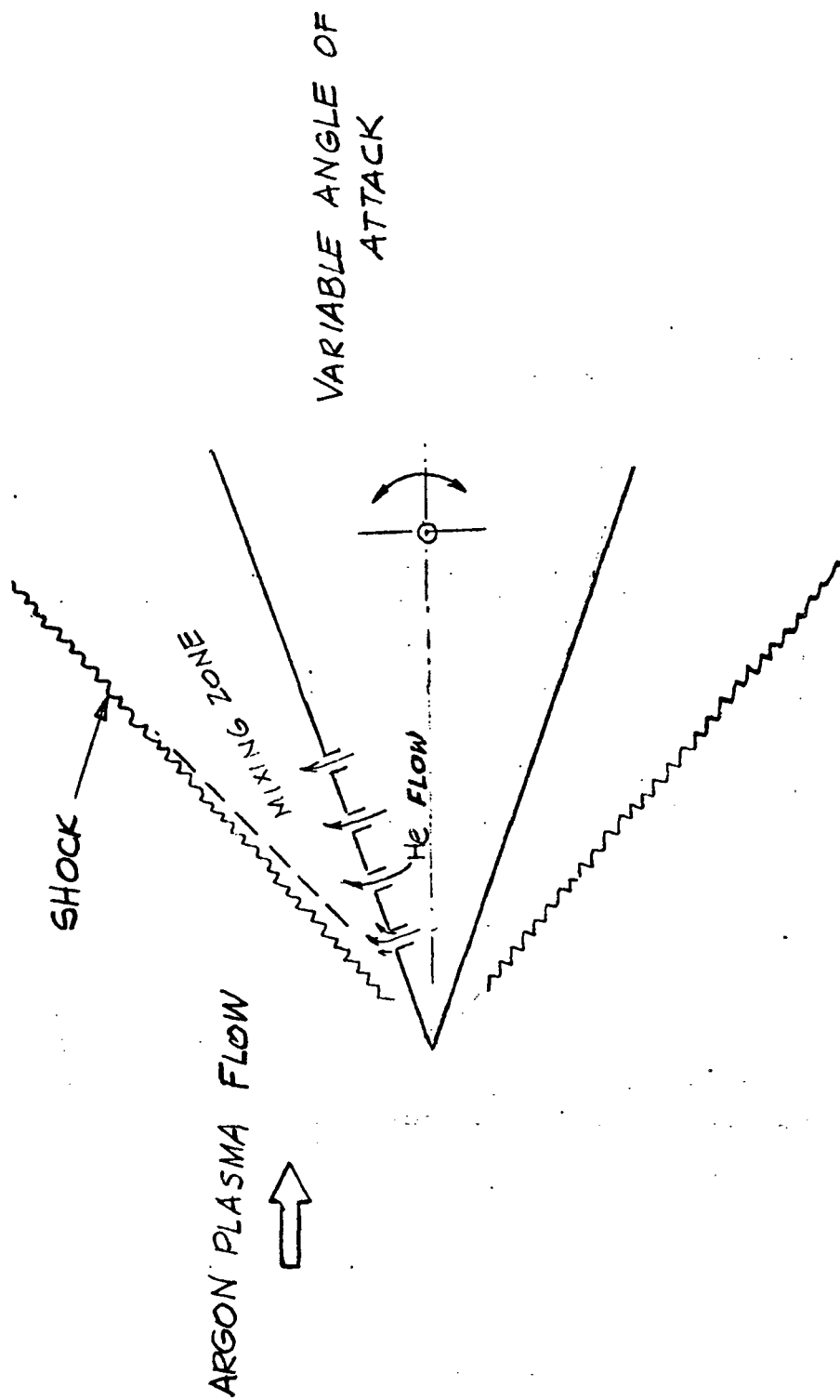


Figure 9. Injection Transverse to Flow

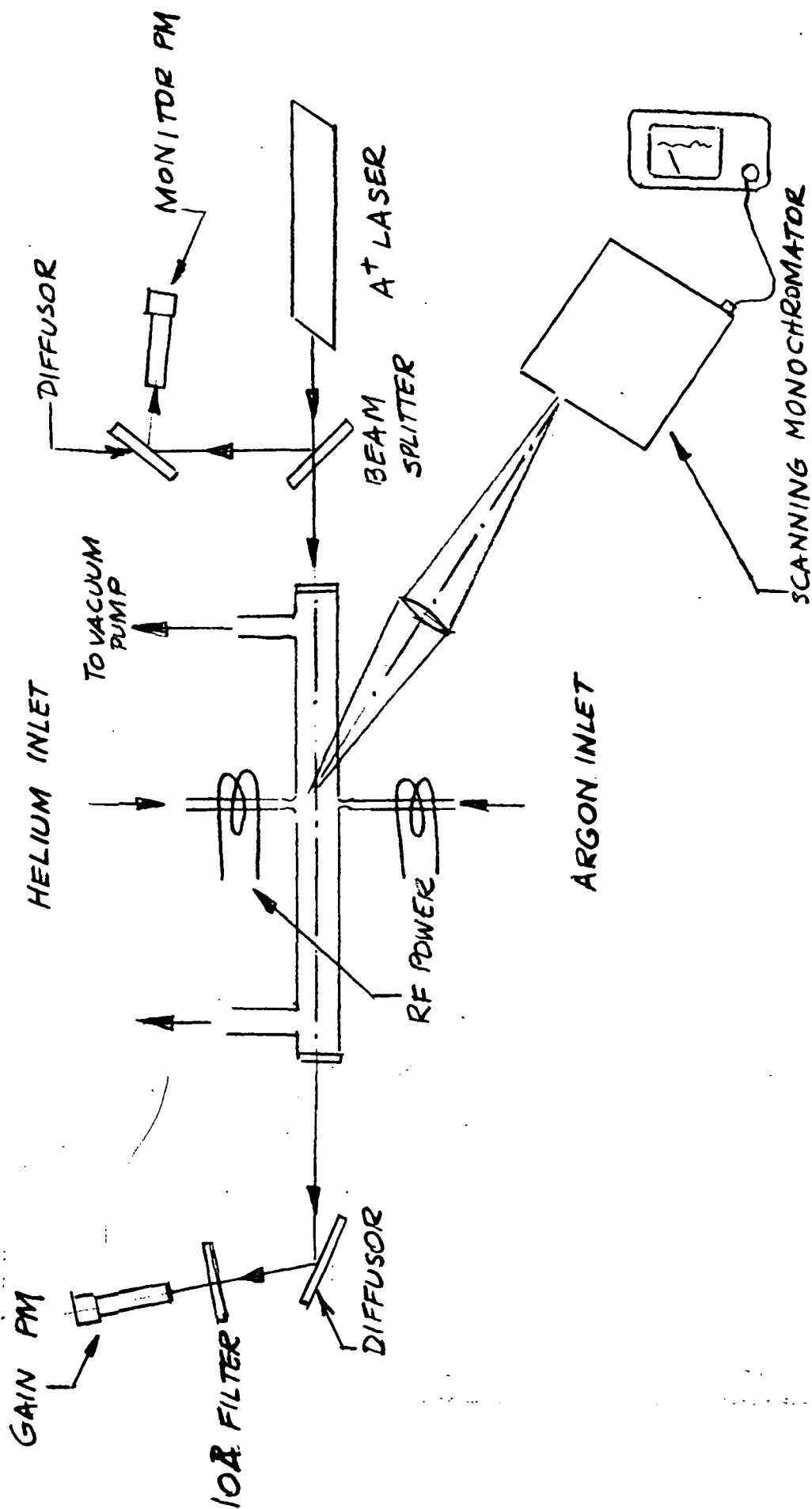


Figure 10. Gain Measurement Apparatus

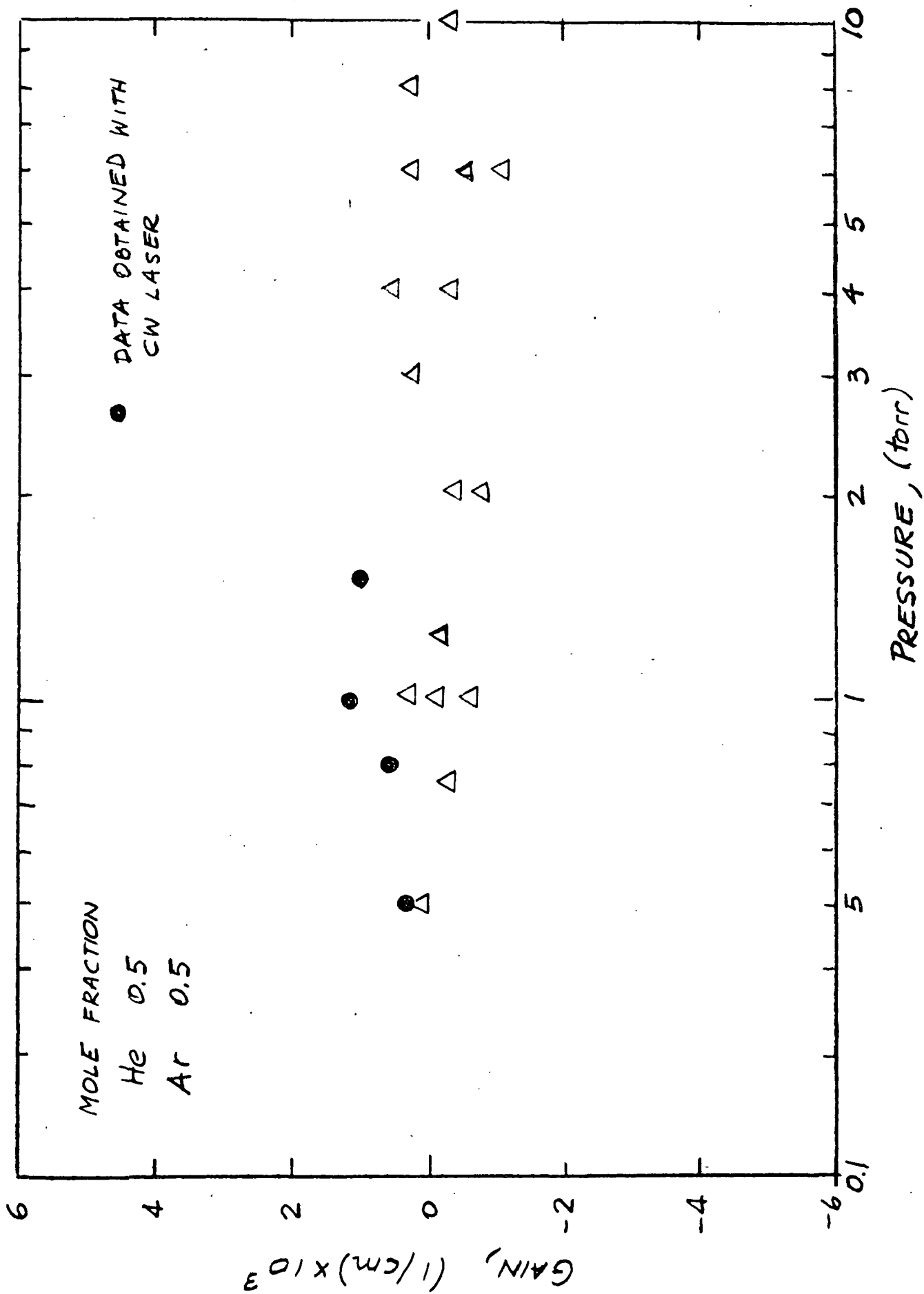


Figure 11. Small Signal Gain vs. Pressure

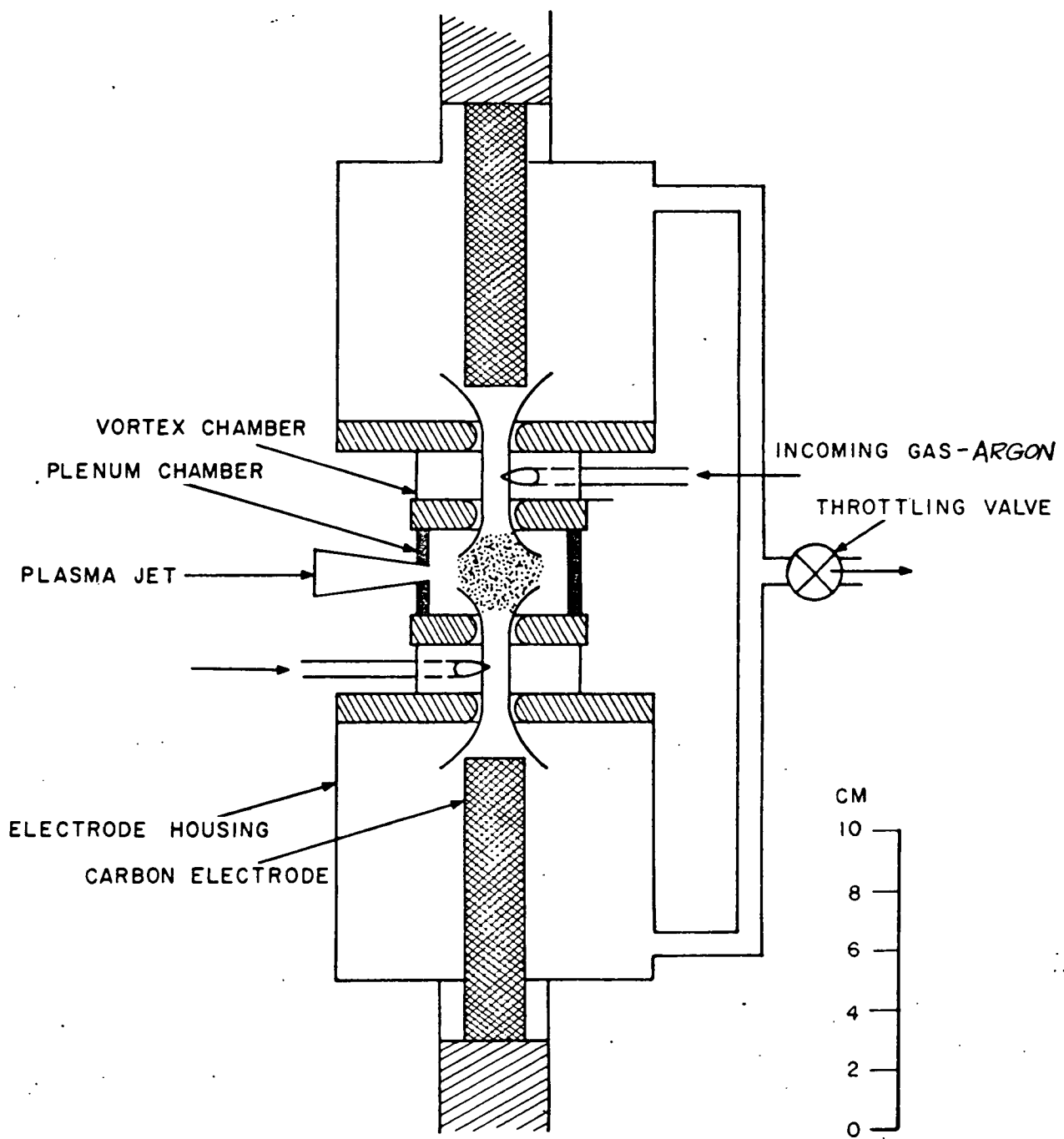


Figure 12. Diagram of Plasma Generator

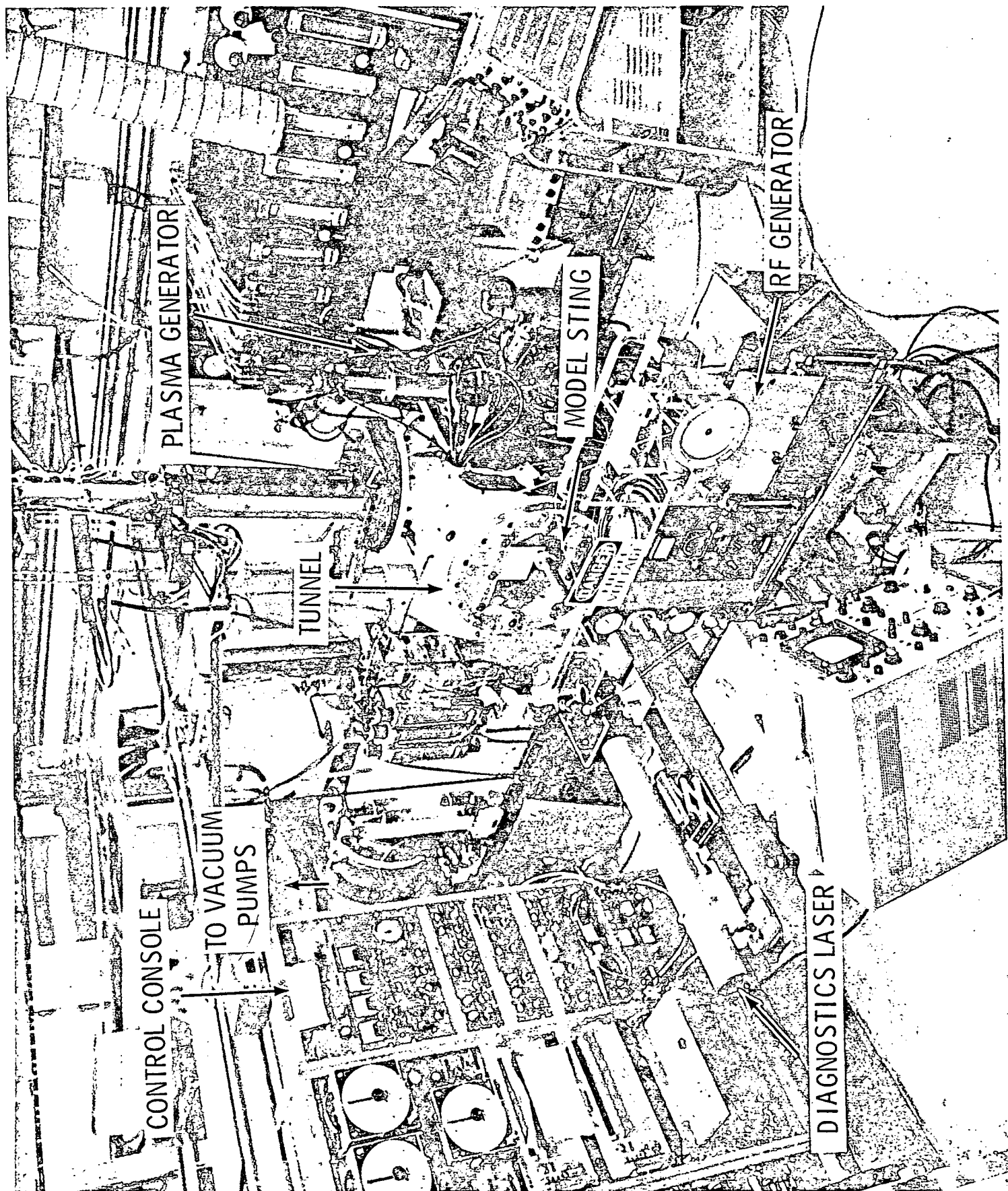


Figure 13. Arc Tunnel Gain Apparatus

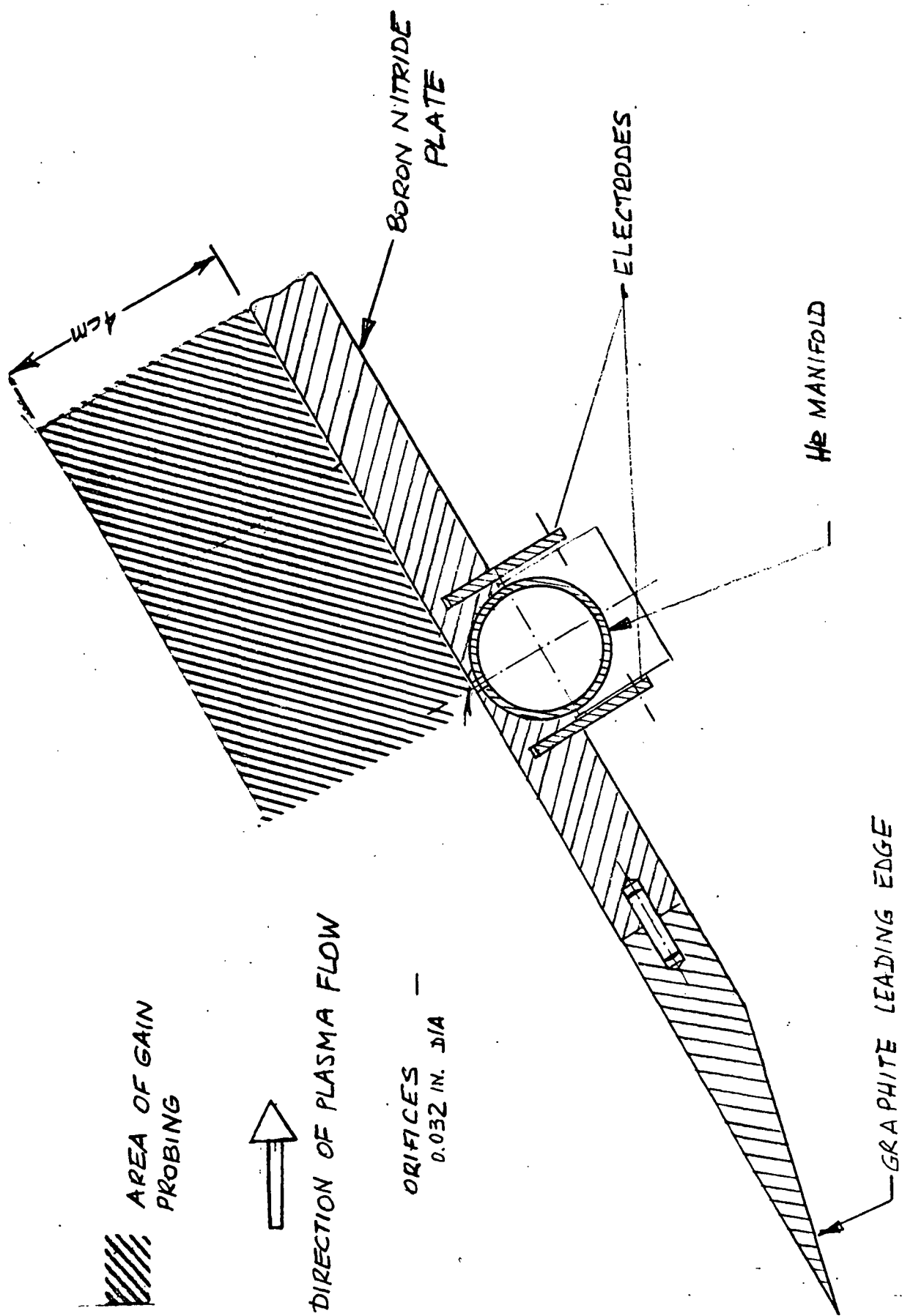


Figure 14. Schematic of Helium Injector

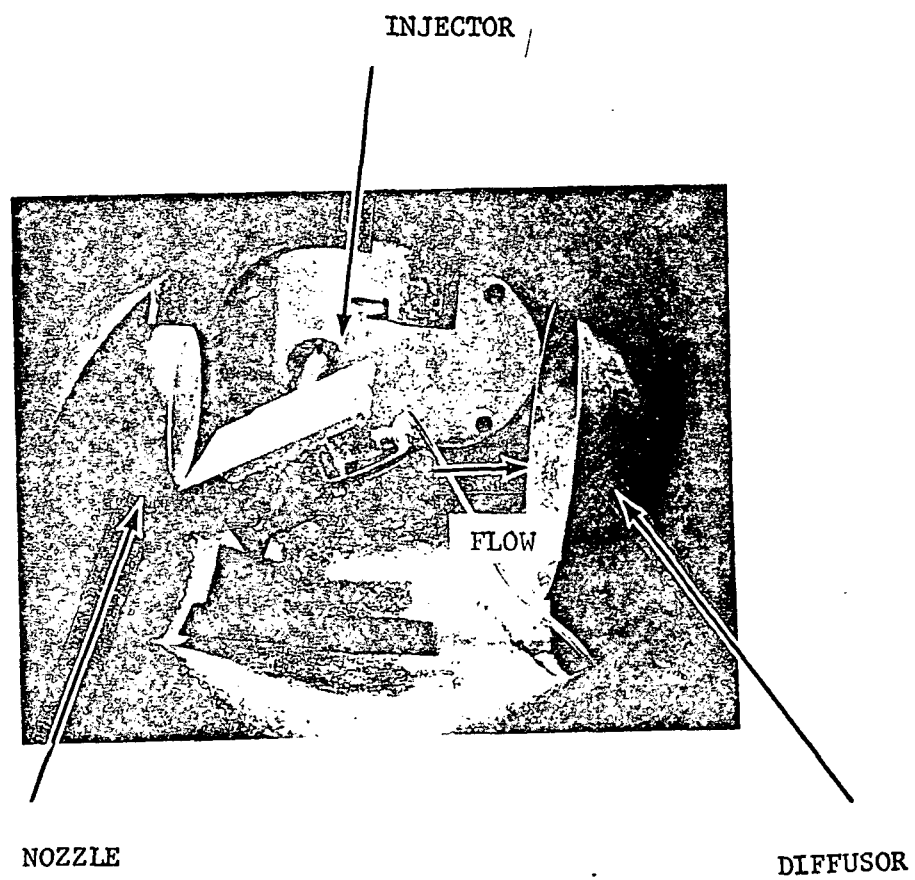


Figure 15. Helium Injector in Arc Tunnel Test Section

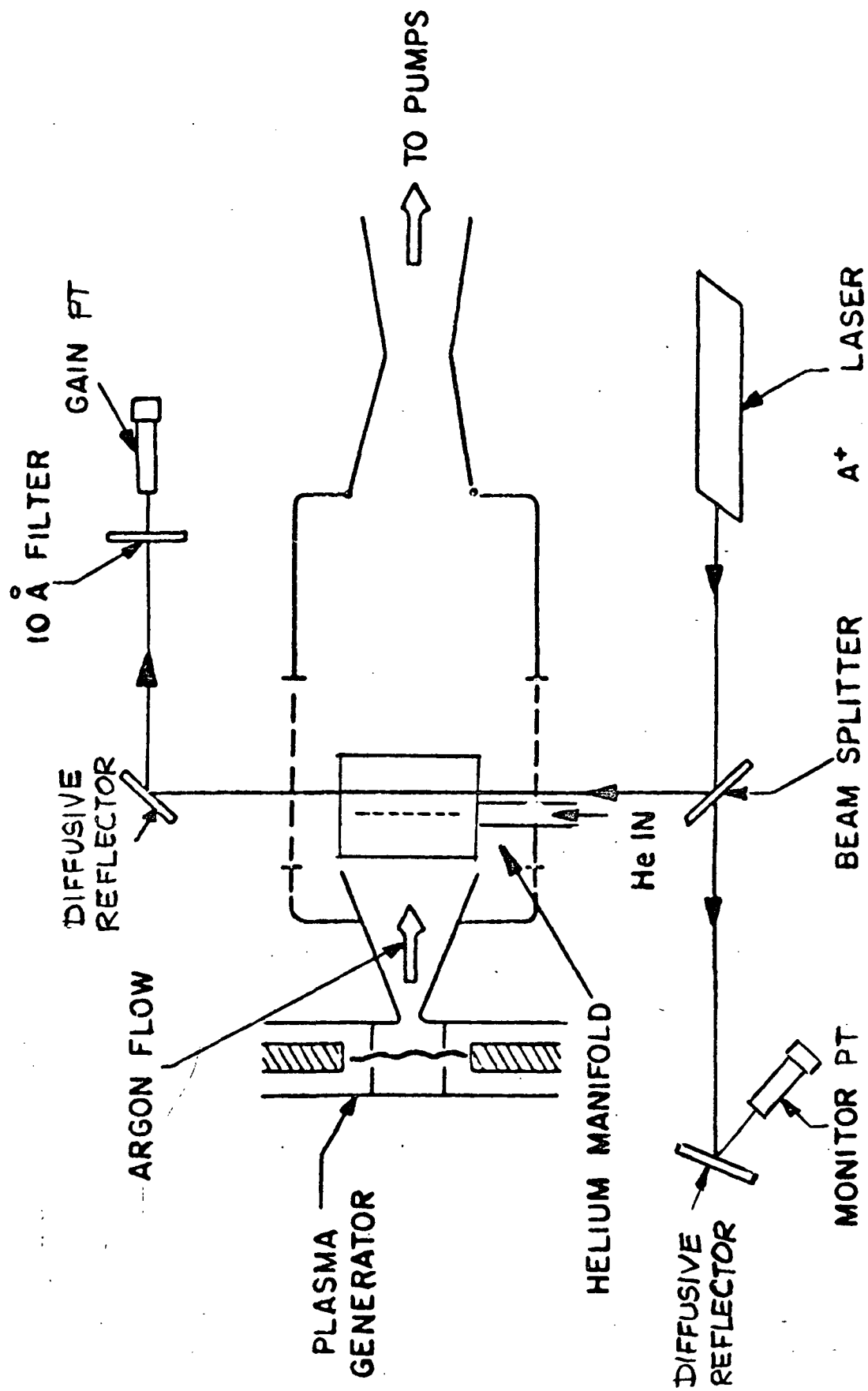


Figure 16. Schematic Diagram of Instrumentation